Lipid-Phase Structure in Epithelial Cell Membranes: Comparison of Renal Brush Border and Basolateral Membranes†

Nicholas P. Illsley,* Herbert Y. Lin,‡ and A. S. Verkman
Cardiovascular Research Institute, University of California, San Francisco, California 94143
Received September 17, 1987; Revised Manuscript Received November 23, 1987

ABSTRACT: The lipid-phase structures of brush border membrane vesicles (BBMV) and basolateral membrane vesicles (BLMV) isolated from rabbit renal cortex were compared by steady-state and phase-modulation measurements of diphenylhexatriene (DPH) and *trans*- and *cis*-parinaric acid (*t*PnA and *c*PnA) fluorescence. A temperature-scanning system was used which gave reproducible temperature profiles of steady-state and dynamic fluorescence parameters with a resolution of 0.1 °C. Steady-state anisotropy of DPH showed a triphasic dependence on temperature with slope discontinuities at 22 ± 4 and 47 ± 3 °C (BBMV) and at 23 ± 2 and 48 ± 1 °C (BLMV). At all temperatures, DPH anisotropy in BBMV was greater than that in BLMV. Ground-state heterogeneity analysis of *t*PnA and *c*PnA fluorescence lifetime data demonstrated the presence of long (>12 ns) and short (<5 ns) lifetime components, interpreted in terms of solid-phase and fluid-phase lipid domains. The fraction of solid-phase phospholipid decreased from 0.9 to 0.1 for BBMV and from 0.7 to 0.3 in BLMV with increasing temperature (10–50 °C). In both membranes, tryptophan–PnA fluorescence energy-transfer measurements showed that membrane proteins were surrounded by a fluidlike phospholipid phase. These results demonstrate the inadequacy of steady-state DPH anisotropy data in defining the structural characteristics of complex biological membranes. Results obtained with the phase-sensitive parinaric acid probes demonstrate major differences in the phase structure of the two opposing cell membranes in both the bulk lipid and the lipid microenvironment around membrane proteins.

The polarized structure of epithelial plasma membranes is of central importance for vectorial transport of solutes and water. In epithelial tissues, the type and amount of lipids and transport proteins contained in the opposing brush border and basal membranes differ widely, reflecting the differences in structural and transport properties between the membranes. It has been suggested that the physical state of the lipid component of these membranes is an important modulator of membrane transport. The transport of water across liposomal, erythrocyte, tracheal, renal, and placental membranes has been shown to be regulated in part by the physical state of the bilayer (Carruthers & Melchior, 1983; Worman et al., 1986; Verkman & Ives, 1986; Illsley & Verkman, 1986). Similarly, nonelectrolyte transport has been shown to depend on such factors as membrane cholesterol content, lipid chain length, and the extent of chain saturation (McElhaney et al., 1970; Poznansky et al., 1976; Fettiplace & Haydon, 1980; Jain & Wagner, 1980).

Lateral-phase separation is one of the factors which has been suggested as influencing membrane permeability. The examination of this facet of transport regulation in biological membranes has been impeded by the difficulty in measuring the phase composition of membranes which contain a variety of phospholipids, which have a high cholesterol content, or which contain large numbers of integral proteins. A number of studies have been carried out examining brush border and basal membranes. These studies have determined the steady-state anisotropy of 1,6-diphenylhexatriene (DPH) or fatty acid anthroyloxy fluorescent probes as a measure of membrane "fluidity". Measurements have been made in renal, tracheal, and intestinal membranes (Verkman & Ives, 1986; LeGrimellec et al., 1982, 1983; Hise et al., 1984; Worman et al., 1986; Brasitus et al., 1985). These reports have concluded that brush border membranes are less fluid than basal membranes and that both membranes appear to undergo some form of thermotropic transition in the 10–50 °C range. In biological membranes, however, DPH is not particularly sensitive to the phase environment, and, as work in this laboratory has demonstrated recently, unless dynamic fluorescence depolarization studies are performed, fluorescence anisotropy data can be misleading (Illsley et al., 1987). In addition, the assignment of a thermotropic transition requires not only that high-resolution data be available but also that some quantitative and systematic method of analysis be used to interpret the temperature dependence of DPH anisotropy (McElhaney, 1978). Finally, DPH anisotropy data cannot be used to distinguish among the possible changes which underlie the transition, such as bulk gel-to-liquid-crystalline phase transition, lipid cluster formation, or changes in lateral-phase separation.

In this paper, we examine the lipid-phase structure of renal brush border and basolateral plasma membranes derived from the rabbit kidney proximal tubule. High-resolution DPH anisotropy data were obtained over the temperature range 10–50 °C. These results are compared with phase separation data obtained from heterogeneity analyses of *cis*- and *trans*-parinaric acid (*c*PnA and *t*PnA, respectively) lifetime data in both membranes. Phase separation data determined from parinaric acid fluorescence in the bulk lipid are also compared with those obtained from probe situated in the microenvironment around membrane proteins.

Materials and Methods

Materials. DPH, *t*PnA, and *c*PnA were obtained from Molecular Probes (Eugene, OR). All other chemicals were

† This work was supported by NIH Grants DK35124, DK07219, and DK39354 and by a grant-in-aid from the American Heart Association. A.S.V. is an established investigator of the American Heart Association.
* Address correspondence to this author at the Cardiovascular Research Institute, 1065 Health Sciences East Tower, University of California, San Francisco, CA 94143.
‡ Present address: Harvard–MIT Division of Health Sciences and Technology, Harvard Medical School, Boston, MA 02115.

0006-2960/88/0427-2077$01.50/0

purchased from Sigma Chemical Co. (St. Louis, MO).

Vesicle Preparation. Rabbit renal cortical brush border and basolateral membranes were prepared and characterized as described previously (Ives et al., 1983; Verkman & Ives, 1986). Brush border membrane vesicles (BBMV) were purified >15-fold relative to homogenate as measured by the activity of maltase, a brush border membrane marker, and <0.3-fold in (Na/K)-ATPase activity, a marker for the basolateral membrane (Chen et al., 1988). Basolateral membrane vesicles (BLMV) were purified >12-fold as measured by assays of (Na/K)-ATPase activity, and less than 0.3-fold with respect to maltase activity (Chen & Verkman, 1988). This preparation is minimally contaminated with other intracellular membranes (Chen & Verkman, 1988). The membranes were resuspended in 250 mM sucrose and 10 mM *N*-(2-hydroxyethyl)piperazine-*N*′-2-ethanesulfonic acid/tris(hydroxymethyl)aminomethane (HEPES/Tris), pH 7.0 (buffer A), and stored at −70 °C. Synthetic phospholipid vesicles were prepared immediately prior to use from dipalmitoylphosphatidylcholine (DPPC) by vigorous vortexing in buffer A (~25 mM) for 1 min at 45 °C.

Probe Incorporation. Vesicles were diluted in N_2-gassed buffer A to concentrations of ~0.1 mg of vesicle protein/mL (BBMV or BLMV) or 250 μM (DPPC vesicles). DPH, *t*PnA, or *c*PnA (2 mM stock in acetone) was added to vesicles to give lipid/dye ratios of >400 (DPH) or >200 (*c*PnA and *t*PnA). Vesicle solutions containing added fluorescent probe (or control samples containing vehicle but no probe) were incubated in the dark under N_2 for 60 min at 23 °C prior to measurement.

Fluorescence Measurements. Fluorescence measurements were performed on samples sealed under N_2 in acrylic or quartz cuvettes. Sample cuvettes were placed in a thermostated cuvette holder, and the samples were stirred continuously by a Teflon-coated magnetic stirring bar at the bottom of the cuvette. Fluorescence intensity, steady-state anisotropy, and three-frequency phase-modulation lifetime measurements were carried out by using an SLM 4800 fluorometer (SLM Instruments, Urbana, IL).

In experiments where temperature was the independent variable, sample temperature was varied by altering the temperature of the water pumped through the cuvette holder. Sample temperature was monitored by a thermistor (YSI 702A, Yellow Springs, OH) sealed into the cuvette and interfaced through a temperature monitor (Cole-Palmer 8502-25, Chicago, IL) to an IBM PC/XT using a Labmaster signal converter (Scientific Solutions Inc., Solon, OH). Sample temperature acquisition was carried out simultaneously with the acquisition of fluorescence data and was used for computer control of the rate of sample heating via analogue signals to the heater/circulator (Haake A80, Haake Inc., Saddle Brook, NJ). The rates of temperature increase generated by this feedback control were linear with respect to time with a small degree of feedback oscillation. In anisotropy experiments, temperature and fluorescence data were collected over 0.25-s intervals and averaged over 10 s, using a rate of temperature increase of 0.6 ± 0.08 °C/min. In fluorescence lifetime experiments, phase, modulation, and temperature data were collected and averaged over 0.4-s intervals.

Steady-state DPH anisotropy was measured by using the T format at an excitation wavelength of 360 nm (excitation scattering <1%) and with a 4-nm band-pass. Fluorescence emission was detected through sequentially placed KV 408 (proximal to sample) and GG 420 Schott glass filters (Duryea, PA). Depolarization caused by emission scattering was corrected as described previously (Illsley et al., 1987), using the equation $\ln (r/r_z) = 1 - KA$, where r is the observed anisotropy, r_z is the anisotropy at zero dilution, A is the sample absorbance in the absence of fluorophore, and K is a proportionality constant dependent on the sample being investigated. K was −0.224 for BBMV and −0.248 for BLMV. Steady-state anisotropy was calculated from the equation:

$$r = \frac{I_{\parallel} - GI_{\perp}}{I_{\parallel} + 2GI_{\perp}} \tag{1}$$

where $I_{\parallel}$ is vertically polarized light, $I_{\perp}$ is horizontally polarized light, and G is the "instrumental" anisotropy or G factor. Emission polarizers were set at 0° and 90°. The G factor was determined with the excitation polarizer at 90°, and sample anisotropy was determined with the excitation polarizer at 0°. To permit continuous determination of sample anisotropy in temperature dependence experiments, the G factor was measured at the beginning and end of the temperature range only. Anisotropy was calculated from eq 1 using G factor values interpolated from a linear fit between the G factors measured at initial and final temperatures. The average final/inital ratio for the G factor was 0.9996 ± 0.0013.

Parinaric acid lifetimes were measured by three-frequency phase-modulation methods as described previously (Illsley et al., 1987) using an excitation wavelength of 320 nm and detecting fluorescence through sequentially placed KV 408 and GG 420 cut-on filters. Phase and modulation data were collected at 6, 18, and 30 MHz and averaged over 0.4-s intervals as temperature was varied (average of 365 points). Lifetimes were calculated from the phase and modulation data using reference measurements carried out at the beginning and end of a temperature run (*t*PnA in hexanol, 1.64 ns, 23 °C; Illsley et al., 1987). Lifetimes were calculated by using a reference value taken from a linear interpolation between the initial and final reference measurements. The mean change in the reference phase angle was 0.6°, and the mean change in modulation was less than 1%, from initial to final measurement. The fluorescence lifetime data were averaged in 1 °C bins, and a weighted heterogeneity analysis of the lifetime data, using the averaged data and standard deviations, was carried out as described previously (Illsley et al., 1987). The preexponential factors (α_i) and lifetimes (τ_i) determined from the heterogeneity analysis were used to calculate the fractional intensity (f_i) of each lifetime (Lakowicz, 1983):

$$f_i = \frac{\alpha_i \tau_i}{\sum \alpha_i \tau_i} \tag{2}$$

These data were further transformed to estimate the mole fraction of probe present as the long-lifetime component (m_s) by normalizing for the changes in quantum yield with temperature in both fluid and solid phases:

$$m_s = \frac{(q_f/q_s)f_1}{(q_f/q_s)f_1 + (1 - f_1)} \tag{3}$$

where q_f/q_s is the quantum yield ratio for PnA in solid/fluid phases. The quantum yield ratios were estimated from measurements in DPPC and palmitoyldocosahexaenoylphosphatidylcholine (PDPC) (Sklar et al., 1979a,b).

Parinaric acid lifetimes were also measured at a single temperature (23 °C) using a multifrequency phase-modulation fluorometer (SLM 48000, SLM Instruments, Urbana, IL). Fluorescence was excited at 325 nm using a HeCd laser (Liconix 4230NB, Sunnyvale, CA; 7.5 mW at 325 nm). Emission was measured as described above. Measurements were made at 15 frequencies in the 2–200-MHz range using

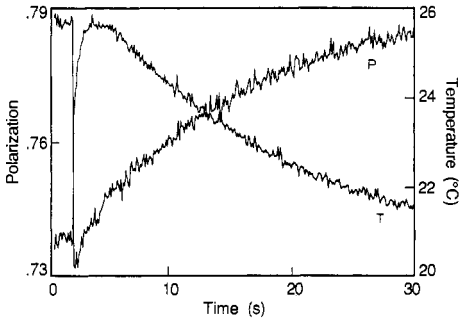

FIGURE 1: Time course of the fluorescence polarization ratio and sample temperature following rapid heating. Changes in $I_{\parallel}/I_{\perp}$ for DPH in BBMV were measured after a rapid increase in solution temperature.

1,4-bis(5-phenyl-2-oxazolyl)benzene (POPOP) in ethanol as a lifetime reference (1.35 ns; Lakowicz et al., 1981). Heterogeneity and distribution analysis was performed by using software provided by SLM Instruments.

Nonradiative energy-transfer measurements were carried out between membrane proteins (excitation at 280 nm) and the parinaric acids to investigate the nature of the lipid environment around proteins. BBMV or BLMV containing either *c*PnA or *t*PnA were excited at 280 nm, and fluorescence emission was detected by using a GG 400 cut-on filter or at 320 nm with a 4-nm band-pass. The "transfer efficiency" (E) was calculated according to the equation:

$$E = \frac{F_{PnA/M}(280/400) - F_M(280/400)}{F_M(280/320)F_{PnA}(320/400)} \quad (4)$$

where $F_{PnA/M}$, F_M, and F_{PnA} are the fluorescence intensities of membrane plus PnA, membrane, and PnA alone, respectively. The numbers in parentheses indicate the excitation and emission wavelengths for each measurement. Data were expressed as the normalized transfer efficiency, $E(T)/E(10\ °C)$. Measurements were carried out over the range 10–50 °C, and the fluorescence data were averaged in 1 °C bins.

RESULTS

Temperature-Induced Membrane Relaxation. A major concern in carrying out temperature dependence experiments was that changes in membrane structure/conformation might be slow events relative to the rate of temperature change. To address this concern, the fluorescence polarization of DPH and *t*PnA was examined in BBMV in response to rapid temperature changes. The ratio of vertically to horizontally polarized light, a measure of fluorescence polarization, was determined by using a T-format configuration. BBMV containing probe were diluted into buffer A and temperature equilibrated in a cuvette into which a thermistor was sealed. At the start of the experiment, an aliquot of buffer A of differing temperature was added and mixed to produce a rapid change in solution temperature. Temperature and fluorescence were measured simultaneously; a typical set of results is shown in Figure 1 for DPH in BBMV. Experiments were carried out with BBMV and BLMV, using both heating and cooling, at a number of initial temperatures. In all cases, changes in fluorescence polarization took place within the mixing time (<2 s) in response to the changes in solution temperature, followed by a slow return to initial values as the temperature reequilibrated.

Steady-State DPH Anisotropy. DPH anisotropy was measured initially in DPPC vesicles as a test of high-resolution fluorescence and temperature data acquisition and for comparison of pure phospholipid membrane anisotropy with that

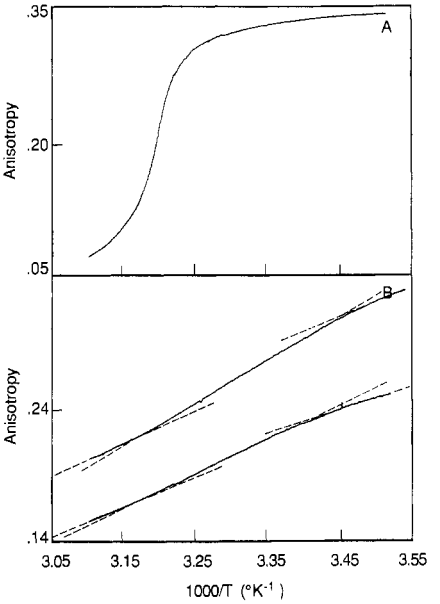

FIGURE 2: High-resolution temperature dependence measurements of DPH steady-state anisotropy. (A) DPH steady-state anisotropy in DPPC vesicles. Plot consists of 398 individual data points. (B) DPH anisotropy in BBMV (upper curve, 383 points) and BLMV (lower curve, 401 points). Dashed lines were drawn according to the triphasic fit of the data as described in the text. Curves are representative of five (BBMV) or four (BLMV) separate renal vesicle preparations.

of biological membranes. DPPC vesicles containing DPH were used to measure anisotropy as temperature was increased from 11 to 50 °C at a rate of 0.6 °C/min. Figure 2A shows a plot of DPH anisotropy against $1/T$ over the temperature range 10–50 °C. The data collected are stable, noise-free, and similar to those obtained elsewhere for DPH in DPPC in terms of the change in anisotropy and the observed transition point [see, for example, Prendergast et al. (1981)].

The steady-state anisotropy of DPH was measured in both BBMV and BLMV over the 10–50 °C temperature range using a heating rate of 0.6 °C/min. The results of one such experiment, typical of four (BLMV) or five (BBMV) separate renal membrane preparations, are shown in Figure 2B, each run comprising an average of 390 points. The data were analyzed by using a nonlinear least-squares fit of the data to models for one, two, or three connected straight lines, where the fitted parameters were the slope(s), y-axis intercept, and intersection points (for the two- or three-line fits).

For the BBMV anisotropy data, four out of the five preparations were best fitted to a triphasic curve with slopes of 0.222 ± 0.013, 0.322 ± 0.028, and 0.240 ± 0.015 ($\times 10^3$ K) and intersection or break points at 22 ± 4 and 47 ± 3 °C (mean ± SD; $n = 4$). The fifth BBMV sample was best fitted to a biphasic curve with a break at 24 ± 2 °C. Analysis of the BLMV anisotropy data in four preparations gave the best fit to triphasic curves with slopes of 0.206 ± 0.005, 0.337 ± 0.060, and 0.248 ± 0.041 ($\times 10^3$ K) and intersection points at 23 ± 2 and 48 ± 1 °C (mean ± SD; $n = 4$). The absolute values of DPH anisotropy in BBMV were consistently higher than those observed for BLMV at the same temperature.

Temperature Dependence of Parinaric Acid Lifetimes. The lifetime of both parinaric acids has been shown to be strongly environment dependent. Thus, in solid-phase lipids, these fluorophores exhibit lifetimes greater than 20 ns which drop to values of 2–5 ns in fluid-phase lipids (Sklar et al., 1977; Wolber & Hudson, 1981; Illsley et al., 1987). The fraction of lipid in solid and fluid phases can be estimated by determining the fraction of fluorescence due to the long-lifetime

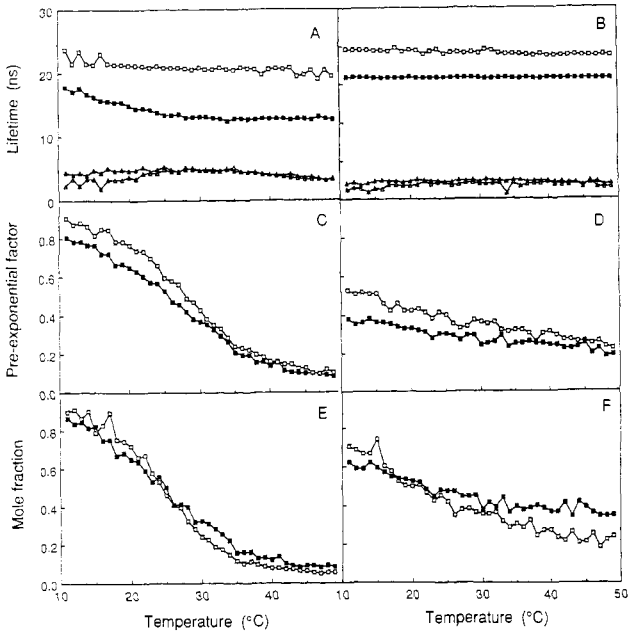

FIGURE 3: Temperature dependence of fluorescence lifetimes, preexponential factors, and mole fractions of the long-lifetime PnA component in BBMV and BLMV. (A) Fluorescence lifetimes (τ_i) for the long (squares) and short (triangles) lifetime components of *t*PnA (open symbols) and *c*PnA (closed symbols) fluorescence in BBMV, calculated from heterogeneity analysis of lifetime data. (B) Fluorescence lifetimes for *t*PnA and *c*PnA in BLMV. (C) Preexponential factors (α_1) for the long-lifetime component of *t*PnA (open squares) and *c*PnA (closed squares) in BBMV, calculated from heterogeneity analysis of lifetime data. (D) Preexponential factors for the long-lifetime component of *t*PnA and *c*PnA in BLMV. (E) Mole fraction (m_s) of *t*PnA (open squares) and *c*PnA (closed squares) present in BBMV as the long-lifetime component determined from heterogeneity analysis of lifetime data (eq 2 and 3 in text). (F) Mole fraction of *t*PnA and *c*PnA present as the long-lifetime component in BLMV.

component. Moreover, while *c*PnA partitions almost equally between solid- and fluid-phase lipids, *t*PnA partitions preferentially into solid-phase lipids by a factor of 3–5 (Sklar et al., 1979a,b; Schroeder, 1983). The partitioning differences can be used to investigate the nature of specific membrane domains, such as the lipid annulus surrounding membrane proteins (see below).

Phase and modulation data were obtained at 6, 18, and 30 MHz as the temperature was raised from 10 to 50 °C (~1.7 °C/min) for *t*PnA and *c*PnA in BBMV and BLMV (average 365 data points per run). The phase and modulation data were converted to phase and modulation lifetimes, averaged in 1 °C bins, and analyzed for ground-state heterogeneity using one- or two-component weighted fits, with or without a scattering (zero lifetime) component. In all cases, the data fitted best to a two-component fit without a significant (<2%) scattering component. In BBMV, the long-lifetime component of *c*PnA fluorescence was 13–17 ns, the long-lifetime *t*PnA component was 20–22 ns, and the short component for both *c*PnA and *t*PnA was 3–5 ns (Figure 3A). In BLMV, the long *c*PnA lifetime was ~16 ns, the long *t*PnA component was 19–20 ns, and the short-lifetime component for both *c*PnA and *t*PnA was 1–2 ns (Figure 3B).

To support the adequacy of a two-component lifetime fit, heterogeneity analysis of multifrequency PnA lifetime data (2–200 MHz) was carried out using two-, three-, and four-component fits. While a three-component fit (χ^2 = 0.7–3.2) was better than a two-component fit (χ^2 = 16–85), no improvement was found with the inclusion of a fourth component (χ^2 = 0.5–1.9). In the three-component fit, the third component was consistently less than 2 ns, and the preexponential factor was less than 4%. The two major components in the three-component fit (>96%) were 5 and 14 ns (*c*PnA in BBMV and BLMV) and 10 and 29 ns (*t*PnA in BBMV and BLMV). The multifrequency data were also analyzed in terms of a distribution of two lifetimes, which gave comparable values for χ^2 (0.8–1.9). For *c*PnA in BBMV, the two lifetimes were centered at 7.4 and 15.1 ns, while for BLMV, the values were 7.3 and 14.1 ns. For *t*PnA, the distributions were centered at 10.6 and 27.7 ns (BBMV) and at 11.1 and 29.3 ns (BLMV). The multifrequency data suggest that the use of a two-component analysis to describe the three-frequency data is correct.

The preexponential factor for the long-lifetime component determined from the heterogeneity analysis (α_1) of the three-frequency data varied with temperature as shown in Figure 3C (BBMV) and Figure 3D (BLMV). These data were transformed to obtain an estimate of the mole fraction of probe demonstrating a long lifetime (m_s, eq 3). In BBMV at 10 °C, more than 85% of both *t*PnA and *c*PnA was in an environment which produced a long fluorescence lifetime; however, this dropped markedly between 20 and 35 °C to leave only 5–10% of the probe in this state above 40 °C. In BLMV, by contrast, both probes showed lower initial values for m_s (60–70%), but the decrease in m_s with increasing temperature was more gradual.

Protein Lipid Environment. The parinaric lifetime data determined above are an average over the entire membrane and as such do not provide information on the microenvironment existing around membrane proteins. An understanding of the environment of proteins is important since the physical state of a membrane can modulate protein functions (Brasitus et al., 1986; Carruthers & Melchior, 1986; Illsley et al., 1987). A number of reports have suggested that membrane proteins are surrounded by an annulus of disordered, fluidlike lipid (Kimelman et al., 1979; Sklar et al., 1979a,b; Blazyk et al., 1985). To examine the membrane regions around proteins in BBMV and BLMV, nonradiative fluorescence energy transfer between protein tryptophan and PnA was measured. If a fluid lipid annulus exists around proteins, then it is reasoned that the energy-transfer efficiency of tryptophan to *t*PnA would increase with temperature, whereas that for *c*PnA would remain the same or decrease with temperature. Increasing temperature would therefore result in an increasing fraction of fluid-phase phospholipid, causing redistribution of *t*PnA from solid to fluid phases, and thus a higher *t*PnA concentration in the annular lipids surrounding proteins. The presence of a fluidlike lipid annulus would predict an increase in the efficiency of tryptophan–*t*PnA transfer with increasing temperature. The opposite prediction would hold if solid-phase phospholipids surrounded membrane proteins.

Figure 4 shows plots of transfer efficiency with temperature for *c*PnA and *t*PnA in BBMV and BLMV, both normalized to unity at 10 °C. The efficiency of transfer to *t*PnA increased 1.5-fold (BBMV) to 3-fold (BLMV) over the temperature range, while the efficiency of transfer to *c*PnA decreased by ~70% in both membranes.

Discussion

Investigations of epithelial brush border and basolateral membranes carried out previously have generally used steady-state fluorescence anisotropy as a measure of fluidity. These studies have for the most part concluded that biphasic or triphasic temperature dependences are indicative of a thermotropic phase transition (LeGrimellec et al., 1982, 1983; Brasitus & Dudeja, 1985; Worman et al., 1986). Previous DPH anisotropy data from this laboratory in renal brush

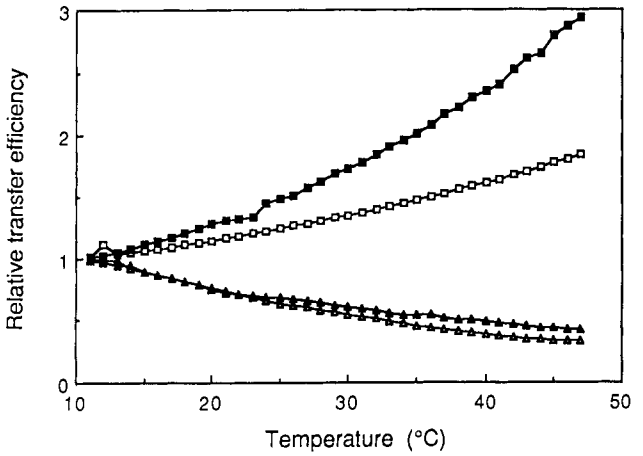

FIGURE 4: Temperature dependence of the efficiency of protein to parinaric acid fluorescence energy transfer. Efficiency of protein to *t*PnA (squares) or *c*PnA (triangles) energy transfer in BBMV (open symbols) or BLMV (closed symbols), normalized to unity at 10 °C.

border and basolateral membranes, however, were deemed insufficient to make this determination (Verkman & Ives, 1986). In more recent work, the attribution of a phase transition in placental brush border vesicles was made only on the basis of combined anisotropy, dynamic depolarization, and lifetime analyses (Illsley et al., 1987). The measurements of DPH anisotropy made here were intended to examine whether high-resolution temperature dependence data could provide any insight into the suggested differences between renal brush border and basolateral membranes (LeGrimellec et al., 1982, 1983; Hise et al., 1984; Molitoris et al., 1985).

One of the concerns with regard to temperature dependence measurements was that the adjustment or relaxation of a membrane following a temperature increment might be a slow event relative to the rate of temperature change. The "temperature jump" experiments described here demonstrate that the relaxation of membrane structure following a temperature perturbation takes place in less than 2 s, as judged by kinetic measurements of DPH or PnA fluorescence anisotropy. Therefore, rapid heating rates should not distort the changes in membrane configuration as reported by fluorescent probes used here.

The absolute values of anisotropy determined from this analysis are similar to those measured by Le Grimellec et al. for human, dog, and rabbit renal membranes at 25 and 37 °C (LeGrimellec et al., 1982, 1983) but differ substantially from those measured in rat renal membranes (Hise et al., 1984; Molitoris et al., 1985) and previous measurements in rabbit renal membranes (Verkman & Ives, 1986). These differences may be due to a lack of correction to zero dilution for emission scattering (Lentz et al., 1979). Over the entire 10–50 °C temperature range, brush border anisotropies measured here were higher than those for basolateral membranes. Analysis of the anisotropy data by a nonlinear least-squares fitting procedure showed the existence of a triphasic curve shape for all but one of the membrane samples, with similar values for the discontinuities or break points (22 ± 4 and 47 ± 3 °C, BBMV; 23 ± 2 and 48 ± 1 °C, BLMV; mean ± SD). The lower temperature discontinuity was found at values similar to those determined by LeGrimellec et al. for the dog kidney brush border and basolateral membranes (LeGrimellec et al., 1982). They did not, however, quantitate the upper temperature inflection point, although they noted a possible change in slope at ~37 °C. The triphasic anisotropy temperature dependences suggest the existence of a phase transition, but due to the composite nature of the anisotropy parameter (containing probe lifetime, rotational, and lipid order information), these data are not sufficient to prove the existence of a thermotropic transition, as shown previously (Illsley et al., 1987). High-resolution temperature dependence data and a systematic method of analysis are necessary to provide reproducible slopes and discontinuities in DPH steady-state anisotropy curves. This is the first report in which well-defined break points, determined reproducibly with a nonlinear fit, have been demonstrated in renal membranes at both the beginning and end of a possible phase transition. Despite this, the information obtained does not prove the existence of a phase transition nor does it give any clue to cause(s) of the slope discontinuities. Heterogeneity analysis of parinaric acid lifetimes was used to investigate possible phase transitions in BBMV and BLMV.

The PnA data indicate that solid and fluid lipid-phase phospholipids coexist over a wide range of temperatures in both BBMV and BLMV. A marked difference between BBMV and BLMV is apparent in the initial proportions of solid- and fluid-phase lipids. Equally noticeable is the change in the proportions of solid- and fluid-phase lipids with temperature in BBMV compared to that observed for BLMV. While the phase state in BBMV changed from predominantly solid phase to a majority of fluid-phase lipid over the 40 °C temperature range, lipids in BLMV were more evenly distributed between the two phase states at 10 °C, and there was less decrease in the solid/fluid ratio with increasing temperature. The lifetimes and change in α_1 observed for BBMV are very similar to those seen previously with PnA in another brush border membrane, human placental microvillous vesicles (Illsley et al., 1987).

It is well established that, secondary to phospholipid composition, lipid structural order is largely determined by the membrane content of cholesterol and sphingomyelin (Yeagle, 1985; Van Blitterswijk et al., 1987). Data for renal membranes show that the cholesterol/phospholipid and sphingomyelin/phospholipid ratios are elevated in BBMV compared to BLMV, while the membrane protein content in BLMV is lower (Chauhan et al., 1982, 1983; Hise et al., 1984; Molitoris et al., 1985; Molitoris & Simon, 1985; Chesney et al., 1986). The differences observed may result not only from the reduction in membrane fluidity by cholesterol but also from the influence of sphingomyelin in amplifying the ordering behavior of cholesterol (Van Blitterswijk et al., 1987). In addition, it appears that the membrane protein content affects the structure of both brush border and basolateral membranes. Removal of protein decreases anisotropy in both types of membrane, but the effect is much more marked for the basolateral membrane (LeGrimellec et al., 1982; Hise et al., 1984). Thus, the changes in membrane structure reported by phase-sensitive probes such as the parinaric acids are likely to be a result of compositional factors.

The value of α_1 for *t*PnA was consistently higher than that for *c*PnA in both BBMV and BLMV, as predicted from the partition data reported previously (Sklar et al., 1979a,b; Schroeder, 1983). No major or consistent differences were present, however, between mole fraction values calculated for *t*PnA and *c*PnA in either BBMV or BLMV. In both cases, the mole fraction of *t*PnA representing the long-lifetime component (m_s) was initially greater than that for *c*PnA, but with increasing temperature, m_s for *t*PnA dropped below that for *c*PnA. In calculating m_s, values for the quantum yield of *t*PnA and *c*PnA in solid and fluid phases were taken from literature values measured in synthetic phospholipid vesicles (Sklar et al., 1979a,b). The contrast between the behavior expected from previously observed partition data and the

crossover of *t*PnA and *c*PnA m_s values suggests that the quantum yield data measured in synthetic phospholipid membranes are not a particularly good estimate of the quantum yield values in these membranes. It is likely that decreases in PnA quantum yield with temperature will be lower in biological membranes than that observed in the pure phospholipid membranes (Kimelman et al., 1979). Thus, *t*PnA m_s values are likely to remain above those for *c*PnA over the entire temperature range. The use of quantum yields determined in synthetic phospholipid vesicles provides the only means at present of estimating the mole fraction of probe in solid and fluid phases which is an interpretable parameter, unlike the preexponential factors (α_i) or fractional intensities (f_i). Despite these difficulties, it is clear that the degree of lateral-phase separation and the changes with temperature differ markedly between BBMV and BLMV.

In the PnA fluorescent lifetime experiments, when the samples being investigated are biological rather than synthetic membranes, containing multiple phospholipid and neutral lipid species, sterols, and proteins, heterogeneity analysis is likely to be an oversimplification of the true domain assembly. Both lifetimes can be analyzed by a distribution of lifetimes (see Results), each distribution possibly corresponding to compositionally differing domains with the same phase state (Fiorini et al., 1987). Nevertheless, heterogeneity analysis of the three-frequency PnA lifetime data provides a reasonable description of membrane lateral-phase separation which is not obtainable by other methods. Studies by Parasassi et al. (1984) and recent work by James et al. (1987) have suggested multiple PnA lifetimes in a variety of systems. The use of two major components in the PnA lifetime analysis of renal BBMV and BLMV was supported, however, by multifrequency analysis using either discrete lifetime values or a distribution of lifetimes. Previous evidence from this laboratory showed that the phase sensitivity of PnA fluorescence lifetimes corresponds closely to the apparent modulation of membrane protein function by phase separation (Illsley et al., 1987).

In light of the changes in lateral-phase separation described above, it is likely that increased quantities of *t*PnA partition into fluid-phase lipid as the amount of solid-phase lipid is reduced at higher temperatures. The fluorescence energy-transfer experiments show that the efficiency of transfer from protein to *t*PNA increased with temperature. We interpret this as an increase in the relative amount of *t*PnA in the immediate environment of proteins as temperature is increased. It is possible that the observed changes are due to alterations in the water/lipid partition coefficient or the dipole/dipole orientation factor; however, the changes in the water/lipid partition coefficient necessary to produce the observed temperature dependence of protein–*t*PnA energy transfer would be quite high (5–10-fold). The heterogeneity of the renal brush border and basolateral membrane proteins makes an alteration in orientation factor also unlikely to be responsible for the changes in energy transfer. The changes observed for *c*PnA are complementary to those seen with *t*PnA. It appears, therefore, that membrane proteins in both BBMV and BLMV are surrounded by a layer of fluidlike lipid. The differences in the extent of the changes in energy-transfer efficiency between BBMV and BLMV suggest variability in the composition and/or nature of the lipid annulus. Electron spin resonance and fluorescence studies have suggested the existence of a disordered area in the vicinity of membrane proteins (Kimelman et al., 1979; Lentz et al., 1983; East et al., 1985; Blazyk et al., 1985; Pates & Marsh, 1987), a finding consistent with the results reported here.

The anisotropy results reported here and elsewhere suggest that BBMV are more fluid than BLMV at all temperatures within the 10–50 °C range. If the changes in anisotropy observed here were due solely to alterations in phase separation, then it might be expected that the changes in DPH steady-state anisotropy in the two membranes would follow a pattern similar to that found for m_s for the parinaric acids. The fact that this does not occur supports the contention that steady-state anisotropy is a complex parameter which is affected by phospholipid composition, saturation, and sterol content (van Blitterswijk et al., 1987) and is not in itself an adequate measure of phase or domain structure. The comparison of the opposing brush border and basolateral epithelial membranes shows major differences between them in the patterns of their lateral-phase separation. BLMV undergo a gradual decrease in the solid/fluid ratio from >1.5 to <0.5 with increasing temperature while BBMV are subject to a major alteration in the solid/fluid ratio from ~9 at 10 °C to <0.1 at 50 °C. Previous literature suggests that phase structure can be an important determinant of membrane protein function. These results suggest new directions for exploring the links between membrane structure and function.

REFERENCES

Blazyk, J., Wu, C.-J., & Wu, S.-C. (1985) *J. Biol. Chem. 260*, 4845–4849.

Brasitus, T. A., & Dudeja, P. K. (1985) *Biochim. Biophys. Acta 819*, 10–17.

Brasitus, T. A., Dudeja, P. K., Worman, H. J., & Foster, E. S. (1986) *Biochim. Biophys. Acta 855*, 16–24.

Carruthers, A., & Melchior, D. L. (1983) *Biochemistry 22*, 5797–5807.

Carruthers, A., & Melchior, D. L. (1986) *Trends Biochem. Sci. (Pers. Ed.) 11*, 331–335.

Chauhan, V. P. S., & Kalra, V. K. (1983) *Biochim. Biophys. Acta 727*, 185–195.

Chauhan, V. P. S., Sikka, S. C., & Kalra, V. K. (1982) *Biochim. Biophys. Acta 688*, 357–368.

Chen, P.-Y., & Verkman, A. S. (1988) *Biochemistry 27*, 655–660.

Chen, P.-Y., Illsley, N. P., & Verkman, A. S. (1988) *Am. J. Physiol. 254*, F114–F120.

Chesney, R. W., Gusowski, N., & Zelikovic, I. (1986) *Pediatr. Res. 20*, 1305–1309.

East, J. M., Melville, D., & Lee, A. G. (1985) *Biochemistry 24*, 2615–2623.

Fettiplace, R., & Haydon, D. A. (1980) *Physiol. Rev. 60*, 510–550.

Fiorini, R., Valentino, M., Wang, S., Glaser, M., & Gratton, E. (1987) *Biochemistry 26*, 3864–3870.

Hise, M. K., Mantulin, W. W., & Weinman, E. J. (1984) *Am. J. Physiol. 247*, F434–F439.

Illsley, N. P., & Verkman, A. S. (1986) *J. Membr. Biol. 94*, 267–278.

Illsley, N. P., Lin, H. Y., & Verkman, A. S. (1987) *Biochemistry 26*, 446–454.

Ives, H. E., Yee, V. J., & Warnock, D. G. (1983) *J. Biol. Chem. 25*, 13513–13516.

Jain, M. K., & Wagner, R. C. (1980) in *Introduction to Biological Membranes*, pp 117–142, Wiley, New York.

James, D. R., Turnbull, J. R., Wagner, B. D., Ware, W. R., & Petersen, N. O. (1987) *Biochemistry 26*, 6272–6277.

Kimelman, D., Tecoma, E. S., Wolber, P. K., Hudson, B. S., & Wickner, W. T. (1979) *Biochemistry 18*, 5874–5880.

Lakowicz, J. R. (1983) in *Principles of Fluorescence Spectroscopy*, pp 51–91, Plenum, New York.

Lakowicz, J. R., Cherek, H., & Balter, A. (1981) *J. Biochem. Biophys. Methods 5*, 131–146.
LeGrimellec, C., Giocondi, M.-C., Carriere, B., Carriere, S., & Cardinal, J. (1982) *Am. J. Physiol. 242*, F246–F253.
LeGrimellec, C., Carriere, S., Cardinal, J., & Giocondi, M.-C. (1983) *Am. J. Physiol. 245*, F227–F231.
Lentz, B. R., Moore, B. M., & Barrow, D. A. (1979) *Biophys. J. 25*, 489–494.
Lentz, B. R., Clubb, K. W., Barrow, D. A., & Meissner, G. (1983) *Proc. Natl. Acad. Sci. U.S.A. 80*, 2917–2921.
McElhaney, R. N., De Gier, J., & van Deenan, L. L. M. (1970) *Biochim. Biophys. Acta 219*, 245–247.
Molitoris, B. A., & Simon, F. R. (1985) *J. Membr. Biol. 83*, 207–215.
Molitoris, B. A., Alfrey, A. C., Adron Harris, R., & Simon, F. R. (1985) *Am. J. Physiol. 249*, F12–F19.
Parasassi, T., Conti, F., & Gratton, E. (1984) *Biochemistry 23*, 5660–5664.
Pates, R. D., & Marsh, D. (1987) *Biochemistry 26*, 29–39.
Poznansky, M., Tang, S., White, P. C., Milgram, J. M., & Selenen, M. (1976) *J. Gen. Physiol. 67*, 45–66.
Prendergast, F. G., Haugland, R. P., & Callahan, P. J. (1981) *Biochemistry 20*, 7333–7338.
Schroeder, F. (1983) *Eur. J. Biochem. 132*, 509–516.
Silvius, J. R., Read, B. D., & McElhaney, R. N. (1978) *Science (Washington, D.C.) 199*, 902–904.
Sklar, L. A., Hudson, B. S., & Simoni, R. D. (1977) *Biochemistry 16*, 819–828.
Sklar, L. A., Miljanich, G. P., Bursten, S. L., & Dratz, E. A. (1979a) *J. Biol. Chem. 254*, 9583–9591.
Sklar, L. A., Miljanich, G. P., & Dratz, E. A. (1979b) *Biochemistry 18*, 1707–1716.
Van Blitterswijk, W. J., van der Meer, B. W., & Hilkmann, H. (1987) *Biochemistry 26*, 1746–1756.
Verkman, A. S., & Ives, H. E. (1986) *Am. J. Physiol. 250*, F633–F643.
Wolber, P. K., & Hudson, B. S. (1981) *Biochemistry 20*, 2800–2810.
Worman, H. J., Brasitus, T. A., Dudeja, P. K., Fozzard, H. A., & Field, M. (1986) *Biochemistry 25*, 1549–1555.
Yeagle, P. L. (1985) *Biochim. Biophys. Acta 822*, 267–287.

A Fourth Type of Rabbit Protein Kinase C

Shigeo Ohno,[‡] Hiroshi Kawasaki,[‡] Yasuhiko Konno,[‡] Masaki Inagaki,[§] Hiroyoshi Hidaka,[§] and Koichi Suzuki*[,‡]

Department of Molecular Biology, The Tokyo Metropolitan Institute of Medical Science, Hon-Komagome, Bunkyo-ku, Tokyo 113, Japan, and Department of Pharmacology, Mie University School of Medicine, Edobashi, Tsu, Mie 514, Japan

Received August 28, 1987; Revised Manuscript Received October 27, 1987

ABSTRACT: Three rabbit cDNA clones coding for three types of protein kinase C (PKC α, β, and γ) have recently been identified and the structures determined [Ohno, S., Kawasaki, H., Imajoh, S., Suzuki, K., Inagaki, M., Yokokura, H., Sakoh, T., & Hidaka, H. (1987) *Nature (London) 325*, 161–166]. By use of these cloned cDNAs as hybridization probes, a fourth type (δ) of cDNA clone, which encodes a protein highly homologous to PKC α, β, and γ, was identified. PKC δ is composed of 697 amino acid residues and contains several peptide sequences determined at the protein level with the brain PKC preparation. This indicates that this molecular type (PKC δ) is, along with PKC α, β, and γ, a constituent of the brain PKC preparation. Sequence comparison among the four PKC types revealed that PKC δ is somewhat distinct from the other PKC types. PKC δ shows 99% amino acid sequence identity with rat PKC type I [Knopf, J. L., Lee, M.-H., Sultzman, L. A., Kriz, R. W., Loomis, C. R., Hewick, R. M., & Bell, R. M. (1986) *Cell (Cambridge, Mass.) 46*, 491–502], indicating relationship of these PKC types. The mRNA for PKC δ is exclusively concentrated in the brain.

Receptor-mediated hydrolysis of phospholipid is involved in a variety of agonist-specific and cell type dependent stimulus–response systems where protein kinase C (PKC) plays an essential role (Nishizuka, 1986).

We have previously described three distinct types of rabbit cDNA clones that encode closely related proteins (Ohno et al., 1987a). These proteins contain sequences identical with those determined from peptides derived from an apparently homogeneous preparation of rabbit brain PKC and were thus designated PKC α, β, and γ. The presence of a peptide that cannot be accounted for by the three PKC types suggested the existence of an additional type(s) of PKC. Thus, we screened a rabbit cDNA library in an attempt to isolate cDNA clones coding for an additional type of PKC and/or a protein related to PKC under low-stringency hybridization conditions using the cDNA fragments as probes. Here we report the isolation of cDNA clones coding for a protein (PKC δ) that shows complete amino acid sequence identity with several peptide sequences of rabbit PKC. The deduced sequence of PKC δ, in conjunction with those for PKC α, β, and γ, explains all the peptide sequences of rabbit brain PKC determined at the protein level. Comparison of amino acid sequences among PKC types from various species shows that rabbit PKC δ corresponds to rat PKC I (Knopf et al., 1986) and human and bovine PKC γ (Coussens et al, 1986).

Experimental Procedures

Screening of Rabbit Brain cDNA Libraries. Two independent rabbit brain cDNA libraries in λgt10 were constructed

[‡] The Tokyo Metropolitan Institute.
[§] Mie University.

0006-2960/88/0427-2083$01.50/0